# Femtosecond Solvation Dynamics in Different Regions of a Bile Salt Aggregate: Excitation Wavelength Dependence

**Aniruddha Adhikari, Shantanu Dey, Ujjwal Mandal, Dibyendu Kumar Das, Subhadip Ghosh, and Kankan Bhattacharyya***

*Physical Chemistry Department, Indian Association for the Cultivation of Science, Jadavpur, Kolkata 700 032, India*

*Received: November 6, 2007; In Final Form: December 13, 2007*

Solvation dynamics of coumarin 480 (C480) in the secondary aggregate of a bile salt (sodium deoxycholate, NaDC) is studied using femtosecond up-conversion. The secondary aggregate resembles a long (∼40 Å) hollow cylinder with a central water-filled tunnel. Different regions of the aggregate are probed by variation of the excitation wavelength ($\lambda_{ex}$) from 375 to 435 nm. The emission maximum of C480 displays an 8 nm red shift as the $\lambda_{ex}$ increases from 345 to 435 nm. The 8 nm red edge excitation shift (REES) suggests that the probe (C480) is distributed over regions of varied polarity. Excitation at a short wavelength (375 nm) preferentially selects the probe molecule in the buried locations and exhibits slow dynamics with a major (84%) slow component (3500 ps) and a small (16%) contribution of the ultrafast component (2.5 ps). Excitation at $\lambda_{ex}$ = 435 nm (red end) corresponds to the exposed sites where solvation dynamics is very fast with a major (73%) ultrafast component (≤2.5 ps) and relatively minor (27%) slow (2000 ps) component. In sharp contrast to solvation dynamics, the anisotropy decay becomes slower as $\lambda_{ex}$ increases from 375 to 435 nm. It is proposed that the buried locations ($\lambda_{ex}$ = 375 nm) offer lower friction because of the rigid sheetlike structure of the bile salt.

## 1. Introduction

Bile salts are bioactive natural surfactant molecules that are synthesized in the liver and stored in gall bladder. Micellization of bile salts and their interaction with biological membranes play an important role in biliary secretion and solubilization of cholesterol, lipid, bilirubin, fat-soluble vitamins and many other species in living organisms.[1] A bile salt exhibits facial amphiphilicity. The nonplanar bile salt, sodium deoxycholate (NaDC, Scheme 1a) consists of a convex hydrophobic surface (the steroid ring) and a concave hydrophilic surface (hydroxyl groups and carboxylate ions). In a slightly alkaline medium (pH > 7.5), NaDC displays two critical micellar concentrations ($CMC_1$ and $CMC_2$) at 10 and 60 mM, respectively. Above $CMC_1$, primary aggregates are formed that consist of very few (2−10) monomers.[1a] In the primary aggregate, the polar face of NaDC (hydroxyl group and ions) points outward (Scheme 1b). The secondary aggregate (formed at a concentration >60 mM) resembles an elongated hollow cylinder with a central water filled tunnel (Scheme 1b).[1−2] For NaDC, the cylinder is about 40 Å long and radius of the hollow core is ∼8 Å.[2] The microenvironment and binding dynamics of many fluorescent probes in different sites of a bile salt aggregate has been studied extensively.[3−4] Solvation dynamics in the secondary aggregate has been studied earlier using picosecond techniques.[4] The ultrafast component of solvation dynamics in a bile salt aggregate has not been studied before. Further, there has been no effort to study solvation dynamics in different regions of a bile salt aggregate. In this work, we report on a femtosecond study of solvation dynamics in a secondary aggregate of NaDC.

To probe different regions of the bile salt aggregate, we take recourse to excitation wavelength dependence. Several groups have reported earlier that variation of excitation wavelength selects probes in different regions of a heterogeneous organized assembly.[5] Excitation at a short wavelength (blue end) selects probe in a less polar and hydrophobic ("buried") region, and a long wavelength (red end) excites probe in a polar and exposed region. As a result, with increase in the excitation wavelength ($\lambda_{ex}$) the emission maximum exhibits a gradual red shift. This phenomenon is known as red edge excitation shift (REES).[5] The effect of variation of $\lambda_{ex}$ on steady-state emission spectrum has received attention for a long time. Recently, $\lambda_{ex}$ dependence has been applied to study dynamics in different regions of many organized assemblies. For instance, $\lambda_{ex}$ variation has revealed the differences in solvation dynamics in different regions of an ionic liquid,[6a] reverse micelle,[6b] triblock copolymer micelle,[6c] gel,[6d] lipid vesicles,[6e] and polymer-surfactant aggregate.[6f] Fluorescence resonance energy transfer in different regions of a reverse micelle,[7a] and polymer hydrogel[7b] has also been studied using $\lambda_{ex}$ variation. In this work, we apply this method to study solvation dynamics in different regions of a bile salt aggregate. We used coumarin 480 (C480, Scheme 1c) as a fluorescent probe.

It may be recalled that many recent computer simulations also predict that the dynamics may vary markedly from one region to another in the case of a protein,[8] micelle,[9] surfaces,[10] many hydrophobic cavities,[11] and most recently in ionic liquids.[12] Several recent experimental works also indicate variation of dynamics in different regions of micelles and other organized assemblies.[13−16] Because of the importance of regioselectivity in many biological processes, in this work we focus on solvation dynamics in different sites of a bile salt (NaDC) aggregate.

* To whom correspondence should be addressed. E-mail: pckb@mahendra.iacs.res.in. Fax: (91)-33-2473-2805.

10.1021/jp7106445 CCC: $40.75 
Published on Web 02/27/2008

**SCHEME 1: Schematic Representation of (a) Bile Salt, NaDC, (b) Secondary Aggregate of NaDC, and (c) Coumarin 480 (C480)**

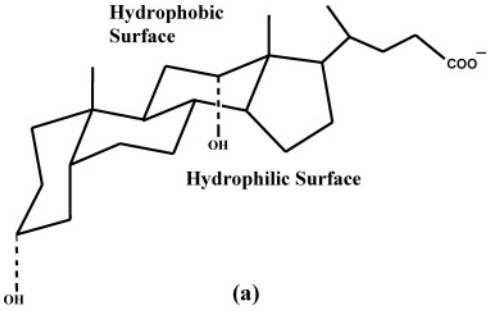


(a)

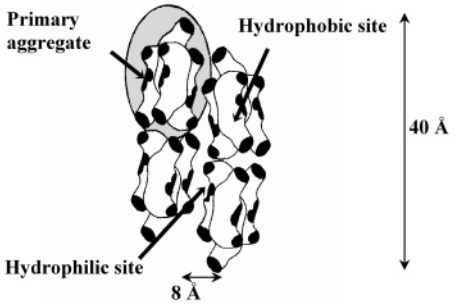


(b)

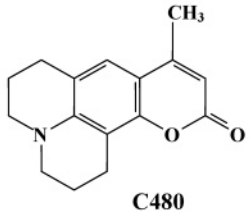


C480

(c)

## 2. Experimental Section

Laser grade coumarin 480 (C480, Exciton) and bile salt sodium deoxycholate (NaDC, Aldrich) were used as received. The steady state absorption and emission spectra were recorded in a Shimadzu UV-2401 spectrophotometer and a Spex FluoroMax-3 spectrofluorimeter, respectively.

In our femtosecond upconversion setup (FOG 100, CDP), the sample was excited at 375, 405, and 435 nm, respectively. Briefly, the sample was excited using the second harmonic of a mode-locked Ti-sapphire laser with an 80 MHz repetition rate (Tsunami, Spectra Physics), pumped by 5 W Millennia (Spectra Physics). The fundamental beam was frequency doubled in a nonlinear crystal (1 mm BBO, $\theta = 25°$, $\phi = 90°$). The fluorescence emitted from the sample was upconverted in a nonlinear crystal (0.5 mm BBO, $\theta = 38°$, $\phi = 90°$) using a gate pulse of the fundamental beam. The upconverted light is dispersed in a monochromator and detected using photon-counting electronics. A cross-correlation function obtained using the Raman scattering from ethanol displayed a full width at half-maximum (fwhm) of 350 fs. The femtosecond fluorescence decays were fitted using a Gaussian shape for the exciting pulse.

To fit the femtosecond data, one needs to know the long decay components. These were detected using a picosecond set up in which the samples were excited at 375, 405, and 435 nm using picosecond laser diodes (IBH Nanoleds) in an IBH Fluorocube apparatus. The emission was collected at a magic angle polarization using a Hamamatsu microchannel plate photomultiplier (5000U-09). The time correlated single photon-counting setup consists of an Ortec 9327 CFD and a Tennelec TC 863 TAC. The data is collected with a PCA3 card (Oxford) as a multichannel analyzer. The typical fwhm of the system response using a liquid scatterer is about 90 ps. The fluorescence decays were deconvoluted using IBH DAS6 software.

To fit the femtosecond transients, we first determined the long picosecond components by deconvolution of the picosecond decays. Then the long picosecond components were kept fixed to fit the femtosecond data. The time-resolved emission spectra (TRES) were constructed using the parameters of best fit to the fluorescence decays and the steady-state emission spectrum following the procedure described by Maroncelli and Fleming.[17a] The solvation dynamics is described by the decay of the solvent correlation function $C(t)$, which is defined as

$$C(t) = \frac{\nu(t) - \nu(\infty)}{\nu(0) - \nu(\infty)} \tag{1}$$

where $\nu(0)$, $\nu(t)$, and $\nu(\infty)$ are the peak frequencies at time 0, t, and ∞, respectively. Note, a portion of solvation dynamics is missed (at $\lambda_{ex} = 405$ and 435 nm) even in our femtosecond set up of time resolution 350 fs. The amount of solvation missed is calculated using the Fee−Maroncelli procedure.[17b] The emission frequency at time zero, $\nu^{p}_{em}(0)$, may be calculated using the absorption frequency ($\nu^{p}_{abs}$) in a polar medium (i.e., C480 in NaDC) as[17b]

$$\nu^{p}_{em}(0) = \nu^{p}_{abs} - (\nu^{np}_{abs} - \nu^{np}_{em}) \tag{2}$$

where $\nu^{np}_{em}$ and $\nu^{np}_{abs}$ denote the steady-state frequencies of emission and absorption, respectively, of the probe (C480) in a nonpolar solvent (i.e., cyclohexane).

To study fluorescence anisotropy decay, the analyzer was rotated at regular intervals to get perpendicular ($I_\perp$) and parallel ($I_{||}$) components. Then the anisotropy function, $r(t)$ was calculated using the formula

$$r(t) = \frac{I_{||}(t) - GI_\perp(t)}{I_{||}(t) + 2GI_\perp(t)} \tag{3}$$

The $G$ value of the picosecond set up was determined using a probe whose rotational relaxation is very fast, for example, coumarin 480 in methanol. The $G$ value was found to be 1.5.

## 3. Results and Discussion

**3.1. Steady-State Absorption and Emission Spectra: $\lambda_{ex}$ Dependence.** All the experiments reported in this work are carried out in 105 mM NaDC. This is well above the $CMC_2$ of NaDC and hence corresponds to a secondary aggregate. In a 105 mM NaDC solution, the absorption maximum of C480 is found to be at 391 nm (Figure 1). This is blue-shifted by 5 nm from the reported absorption maximum (396 nm)[18] of C480 in water. Figure 2 shows the emission spectrum of coumarin 480 in NaDC for various excitation wavelengths ($\lambda_{ex}$). The emission maxima of C480 at different $\lambda_{ex}$ in the secondary aggregate of NaDC are listed in Table 1. Figure 3 shows the $\lambda_{ex}$ dependence of emission maximum of C480 in NaDC. It is readily seen that emission maximum of C480 displays a red shift (REES) of 8 nm from 468 nm at $\lambda_{ex} = 345$nm to 476 nm at $\lambda_{ex} = 435$ nm. The observed REES suggests a distribution of the fluorophore (C480) in different regions of the bile salt. Evidently, excitation at a short wavelength (the blue end, 345 nm), preferentially selects the probes residing at the less polar core region and hence, gives rise to a blue-shifted emission spectrum. At a long $\lambda_{ex}$ (435 nm, red end), probe (C480) molecules in the hydrophilic

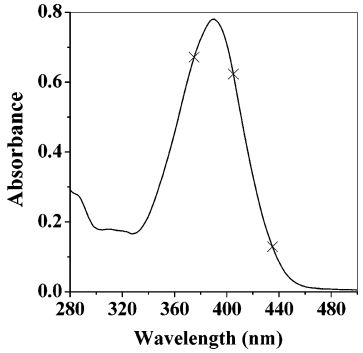


**Figure 1.** Absorption spectrum of C480 in 105 mM NaDC. The excitation wavelengths are marked (×) at 375, 405 and 435 nm.

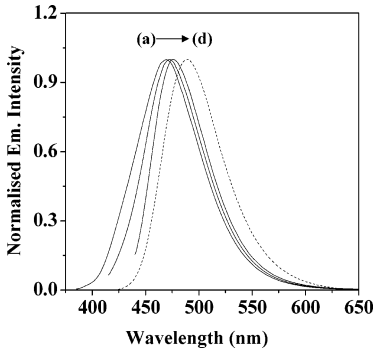


**Figure 2.** Emission spectra of C480 in 105 mM NaDC when excited at (a) 375 nm, (b) 405 nm, (c) 435 nm, and (d) C480 in water (·····) ($\lambda_{ex}$ = 375−435 nm).

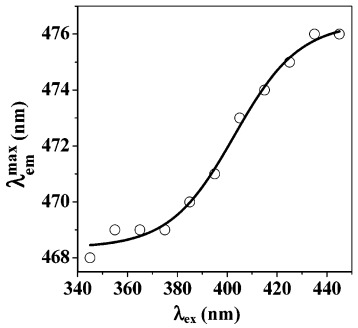


**Figure 3.** Plot of emission maximum of C480 in 105 mM NADC as a function of excitation wavelength.

**TABLE 1: $\lambda_{ex}$ Dependence of Steady-State Emission Maximum and Width (fwhm) of C480 in 105 mM NaDC and Water**

| medium | $\lambda_{ex}$ (nm) | $\lambda_{em}^{max}$ (nm) | fwhm ($cm^{-1}$) |
|---|---|---|---|
| NaDC | 375 | 469 | 3250 |
| NaDC | 405 | 473 | 2900 |
| NaDC | 435 | 476 | 2600 |
| water | 375−425 | 489 | 2600 |

exposed sites are excited almost exclusively, and this leads to a red-shifted emission spectrum.

**3.2. Time-Resolved Studies.** *3.2.1. Solvation Dynamics of C480 in NaDC: $\lambda_{ex}$ Dependence.* Figures 4 and 5 show the picosecond and femtosecond fluorescence transients of C480 in 105 mM NaDC. At the red end of the emission spectrum, a rise precedes the decay, and at the blue end a decay (with no rise) is observed. Such a wavelength dependence of fluorescence decays is a clear indication of solvation dynamics. For $\lambda_{ex}$ = 375 nm (buried site), in NaDC the fluorescence decay at 410 nm (blue end) exhibits four decay components: 3, 126, 950, and 2700 ps. At 540 nm (red end), there are three rise components, 3.5, 260, and 2230 ps, with a long decay component of 7130 ps.

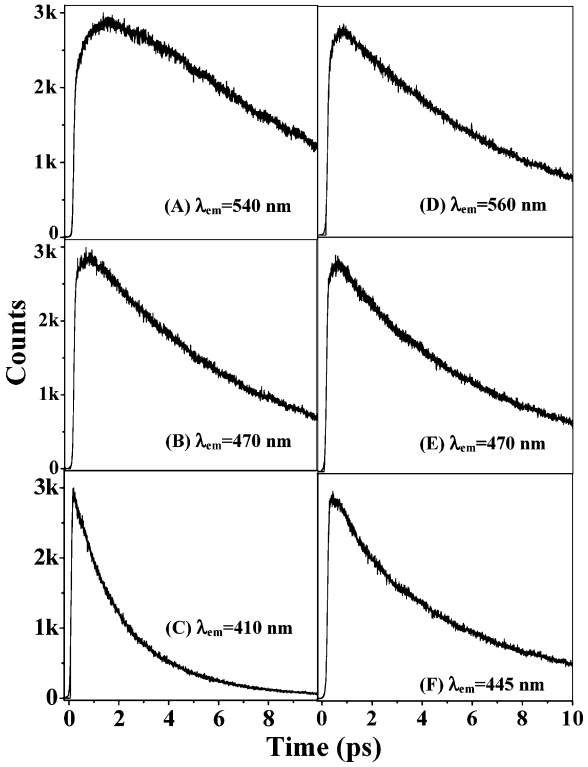


**Figure 4.** Picosecond fluorescence decays of C480 in NaDC at $\lambda_{ex}$ = 375 nm (A−C) and 435 nm (D−F). $\lambda_{em}$ at (A) 540 nm, (B) 470 nm, (C) 410 nm, (D) 560 nm, (E) 470 nm, and (F) 445 nm.

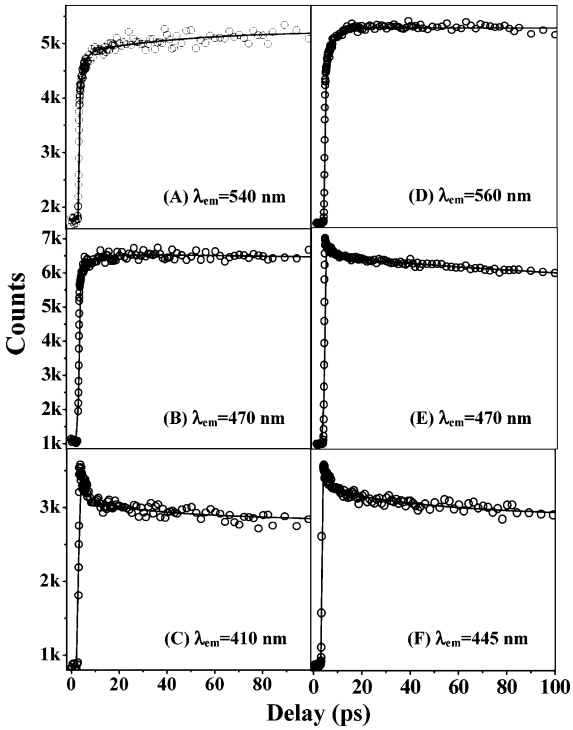


**Figure 5.** Femtosecond fluorescence transients of the C480 in NaDC at $\lambda_{ex}$ = 375 nm (A−C) and 435 nm (D−F). $\lambda_{em}$ at (A) 540 nm, (B) 470 nm, (C) 410 nm, (D) 560 nm, (E) 470 nm, and (F) 445 nm.

For excitation at the red end ($\lambda_{ex}$ = 435 nm), that is, in the polar exposed site, the decay displays two rise components of 2.5 and 690 ps followed by a long decay component of 6800 ps at the red end (560 nm). The fluorescence transient at the

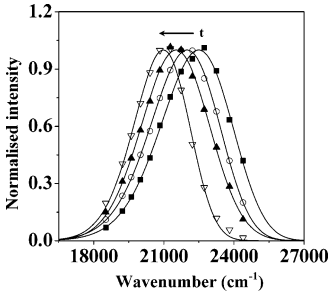


**Figure 6.** TRES of C480 in NaDC at $\lambda_{ex} = 375$ nm at time (A) 0 ps (■), (B) 700 ps (○), (C) 3000 ps (▲), and (D) 12000 ps (▽).

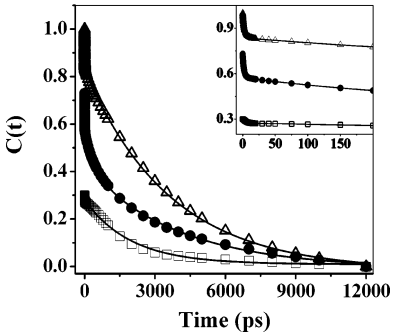


**Figure 7.** Complete decay of the solvent response function $C(t)$ of C480 in NaDC for $\lambda_{ex}$=375 nm (△), $\lambda_{ex}$=405 nm (●), and $\lambda_{ex}$=435 nm (□). The points denote the actual values of $C(t)$, and the solid line denotes the best fit. Initial portions of the decays are shown in the inset.

**TABLE 2: Decay Parameters of $C(t)$ of C480 in NaDC at Different Excitation Wavelengths ($\lambda_{ex}$)**

| $\lambda_{ex}$ (nm) | $\nu$ (0) (cm$^{-1}$) | $\Delta\nu_{obs}$[a] (cm$^{-1}$) | $\tau_1$ ($a_1$) (ps) | $\tau_2$ ($a_2$) (ps) | $\tau_3$ ($a_3$) (ps) | $<\tau_s>$[c] (ps) |
|---|---|---|---|---|---|---|
| 375 | 22500 | 1500 | 2.5 (0.16) | 3500 (0.84) | | 2940 |
| 405 | 22100 | 1100 | <0.3 (0.27)[b], 2.5 (0.15) | 400 (0.15) | 3500 (0.43) | 1570 |
| 435 | 21300 | 500 | <0.3 (0.70)[b], 2.5 (0.03) | 2000 (0.27) | | 540 |

[a] ± 100 cm$^{-1}$. [b] Calculated using Fee−Maroncelli method.[17b] [c] ± 10%.

blue end (445 nm) exhibits three decay components: 4, 870, and 5880 ps.

Figure 6 shows the TRES of C480 in NaDC for $\lambda_{ex} = 375$ nm. From Table 2, it is evident that in NaDC the total dynamic Stokes shift, (DSS = $\nu(0) - \nu(\infty)$), decreases 3 times as $\lambda_{ex}$ increases from 375 to 435 nm. This implies that the solvation dynamics becomes faster with increase in $\lambda_{ex}$.

For $\lambda_{ex} = 375$ nm, that is, for the core or buried region, almost the entire amount of solvation is captured in our femtosecond set up. However, at a long $\lambda_{ex}$ (435 nm), a significant amount of solvation dynamics is missed even in our femtosecond set up. The amount of solvation missed may be calculated by using Fee−Maroncelli procedure.[17b] Figure 7 shows the decays of solvent response function, $C(t)$, for different excitation wavelengths, and Table 2 summarizes the decay parameters of $C(t)$ along with DSS.

From Figures 7 and Table 2, it is evident that for $\lambda_{ex} = 405$ nm, solvation dynamics in NaDC displays a very fast (∼2.5 ps) component, and a very long component (3500 ps) along with an intermediate component (400 ps). For $\lambda_{ex} = 435$ nm, a major part of solvation dynamics is missed in our femtosecond set up (resolution 0.3 ps) and a fast 2.5 ps and a slow 2000 ps component are detected. With increase in $\lambda_{ex}$ from 375 to 435 nm, contribution of the ultraslow component (2000−3500 ps) decreases from 84 to 27% with a concomitant increase in the contribution of the fast component (≤2.5 ps) from 16 to 73%.

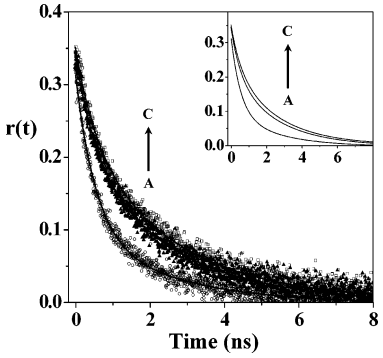


**Figure 8.** Fluorescence anisotropy decays of C480 ($\lambda_{em}$= 460 nm) along with fitted curves in NaDC at (A) $\lambda_{ex} = 375$ nm (○), (B) $\lambda_{ex} = 405$ nm (▲), and (C) $\lambda_{ex} = 435$ nm (□). The fitted curves are shown in the inset.

**TABLE 3: $\lambda_{ex}$ Dependence of Anisotropy Decay of C480 in 105 mM NaDC**

| $\lambda_{ex}$ | $r_0$ | $\tau_{r1}$($a_1$) (ps) | $\tau_{r2}$($a_2$) (ps) | $<\tau_r>_{av}$[a] (ps) |
|---|---|---|---|---|
| 375 | 0.31 | 600 (0.68) | 2800 (0.32) | 1300 |
| 405 | 0.35 | 600 (0.39) | 2800 (0.61) | 1950 |
| 435 | 0.35 | 600 (0.32) | 2800 (0.68) | 2100 |

[a] ± 10%, $<\tau_r>_{av} = a_1\tau_{r1} + a_2\tau_{r2}$

*3.2.2. Fluorescence Anisotropy Decay of C480 in NaDC.* In bulk water, the time constant of fluorescence anisotropy decay of C480 is ∼70 ps.[19] The fluorescence anisotropy decay of C480 in bile salt aggregate (at the blue side of the peak, 460 nm, Figure 8) is found to be much slower and is fitted to a biexponential function

$$r(t) = r_0[\beta \exp(-t/\tau_{slow}) + (1 - \beta) \exp(-t/\tau_{fast})] \quad (4)$$

The high value of initial anisotropy ($r_0 = 0.31$, 0.35, and 0.35 for $\lambda_{ex} = 375$, 405 and 435 nm, respectively) in the bile salt aggregate (Table 3) suggests that our picosecond setup captures almost the entire rotational dynamics in this case. For $\lambda_{ex} = 375$ nm, the anisotropy decay of C480 in NaDC is described by two decay components of 600 ps (68%) and 2800 ps (32%) (Figure 8, Table 3). At $\lambda_{ex} = 435$ nm, the observed components are found to be 600 (32%) and 2800 ps (68%). It is apparent that with increase in $\lambda_{ex}$ the anisotropy decay of C480 in NaDC aggregate becomes slower.

## 4. Discussion

The most important finding of this work is the marked excitation wavelength dependence of the solvation dynamics and anisotropy decay of C480 in NaDC aggregates. Evidently, excitation at a short wavelength (375 nm) selects the probe C480 deep inside the tunnel of the tubular bile salt aggregates. The bile salt (NaDC) has three hydrogen-bonding sites (two hydroxyl groups and the carboxylate ion). These three sites are well separated and hence, the region inside the tunnel is quite hydrophobic. Since the length of the tunnel (∼40 Å) is much longer than the length of the probe C480 (∼12 Å), the probe remains fully buried inside the aggregate. The rigid sheetlike structure of the NaDC molecule and the steric hindrance inside the tunnel shields the probe from bulk water. On the contrary, the probe near the rim ("mouth") of the tunnel is exposed to bulk water molecules.

The observed $\lambda_{ex}$ dependence may be rationalized as follows. At $\lambda_{ex} = 375$ nm, mostly the C480 molecules in the buried locations within the tunnel are excited. In this region, the water molecules are hydrogen bonded to the bile salt molecules and are largely immobilized. The reduced mobility of these water molecules are consistent with the bound-to-free interconversion model.[20] Many recent computer simulations also predict large scale slowing down of water molecules inside micelles, proteins, and supramolecular assemblies.[8−11] The slowness of the water molecules in the buried locations of the bile salt aggregate arises mainly from the need of rupture of hydrogen bond of the bound water molecules and large scale structural reorganization required for solvation dynamics.[20]

Excitation at the red end ($\lambda_{ex} = 435$ nm) selects the C480 in the polar and exposed regions near the mouth of the tunnel. The C480 molecules in this region experience many fast moving water molecules in its immediate vicinity. As a result, the contribution of the fast component (0.3 and 2.5 ps) of solvation dynamics is much higher (73%) at $\lambda_{ex} = 435$ nm than that (16%) at $\lambda_{ex} = 375$ nm. The contribution of the slow component (2000−3500 ps) exhibits a concomitant decrease by a factor of 3 from 84% at $\lambda_{ex} = 375$ nm to 27% at $\lambda_{ex} = 435$ nm.

Interestingly, the anisotropy decay exhibits an opposite trend and becomes 1.5 times slower as $\lambda_{ex}$ increases from 375 to 435 nm. Note, the anisotropy decay arises from rotation of the probe C480 molecules while solvation dynamics arises from motion of the water molecules. The results of the anisotropy decay measurement suggests that the C480 experiences lower friction in the buried site ($\lambda_{ex} = 375$ nm) compared to that in the exposed site ($\lambda_{ex} = 435$ nm). One possible explanation of this interesting observation could be as follows. Inside the bile salt aggregate, the nonplanar sheetlike structure and lack of many hydrogen-bonding sites of the NaDC molecule may give rise to "void" regions with very few water molecules. Thus, part of the probe C480 may experience very small friction. This may make anisotropy decay relatively faster inside the cavity (for $\lambda_{ex} = 375$ nm). It is important to note that the opposite trend in the $\lambda_{ex}$ dependence of solvation dynamics and anisotropy decay indicates that they arise from different kinds of motions.

## 5. Conclusion

This work shows that solvation dynamics and anisotropy decay of C480 in the secondary aggregate of NaDC markedly depends on the excitation wavelength ($\lambda_{ex}$). The $\lambda_{ex}$ dependence is ascribed to different locations (or sites) inside the bile salt aggregate. In the buried location (accessed at $\lambda_{ex} = 375$ nm), solvation dynamics is much slower and anisotropy decay is faster than those in the exposed region (selected at $\lambda_{ex} = 375$ nm). These observations are attributed to the nonplanar rigid structure of the NaDC molecule. The slow solvation dynamics arises from immobilization of the water molecules inside the cavity. The faster anisotropy decay arises from lower friction provided by the nonplanar NaDC molecules inside the cavity. The regio-selectivity of solvation dynamics in the bile salt aggregate may have biological implications (e.g., in site specific reaction and solubilization). A recent simulation by Thompson and co-workers reveal variation of reaction free energy for proton transfer in different regions of a nanocavity.[11b−c]

**Acknowledgment.** Thanks are due to Department of Science and Technology, India (Project Number: IR/I1/CF-01/2002 and J.C. Bose Fellowship) and Council of Scientific and Industrial Research (CSIR) for generous research grants. A.A., S.D., U.M., D.K.D., and S.G. thank CSIR for awarding fellowships.

## References and Notes

(1) (a) Small, D. M. *The Bile Acid*; Plenum: New York, 1971; Vol. 1, p 302. (b) O'Connor, C. J.; Wallace, R. G. *Adv. Colloid Interface Sci.* **1985**, *22*, 1. (c) Borgtstorm, B.; Barrowman, J. A.; Lindstorm, M. In *Sterols and bile acid*; Danielsson, H., Sjoval, J., Eds.; Elsevier: Amsterdam, 1985.

(2) (a) Leggio, C.; Galantini, L.; Zaccarelli, E. *J. Phys. Chem. B* **2005**, *109*, 23857. (b) Hjelm, R. P.; Schteingert, C. D.; Hofman, A. F.; Thiagrajan, P. *J. Phys. Chem. B* **2000**, *104*, 197. (c) Santhanalakshmi, J.; Shantha Lakshmi, G.; Aswal, V. K.; Goyal, P. S. *Proc. - Indian Acad. Sci.* **2001**, *113*, 55. (d) Lopez, F.; Samseth, J.; Mortensen, K.; Rosenqvist, E.; Rouch, J. *Langmuir* **1996**, *12*, 618. (e) Esposito, G.; Giglio, E.; Pavel, N. V.; Zanobi, A. *J. Phys. Chem*. **1987**, *91*, 356.

(3) (a) Megyesi, M.; Biczok, L. *J. Phys. Chem. B* **2007**, *111*, 5635. (b) Yihwa, C.; Quina, F. H.; Bohne, C. *Langmuir* **2004**, *20*, 9983. (c) Waissbluth, O. L.; Morales, M. C.; Bohne, C. *J. Photochem. Photobiol*. **2006**, *82*, 1030. (d) Gouin, S.; Zhu, X. X. *Langmuir* **1998**, *14*, 4025. (e) Ju, C.; Bohne, C. *J. Phys. Chem.* **1996**, *100*, 3847.

(4) Sen, S.; Dutta, P.; Mukherjee S.; Bhattacharyya, K. *J. Phys. Chem. B* **2002**, *106* 7745.

(5) (a) Demchenko, A. P. *Biophys. Chem*. **1982**, *15*, 101. (b) Lakowicz, J. R. *Biochemistry* **1984**, *23*, 3013. (c) Kelkar, D. A.; Chattopadhyay, A. *J. Phys. Chem. B* **2004**, *108*, 12151. (d) Mukherjee, S.; Chattopadhyay, A. *Langmuir* **2005**, *21*, 287.

(6) (a) Adhikari, A.; Sahu, K.; Dey, S.; Ghosh. S.; Mandal, U.; Bhattacharyya, K. *J. Phys. Chem. B* **2007**, *111*, 12809. (b) Satoh, T.; Okuno, H.; Tominaga, K.; Bhattacharyya, K. *Chem. Lett.* **2004**, *33*, 1090. (c) Sen, P.; Ghosh, S.; Sahu, K.; Mondal, S. K.; Roy, D.; Bhattacharyya, K. *J. Chem. Phys.* **2006**, *124*, 204905. (d) Ghosh. S.; Adhikari, A.; Mandal, U.; Dey, S.; Bhattacharyya, K. *J. Phys. Chem. C* **2007**, *111*, 8775. (e) Sen, P.; Satoh, T.; Bhattacharyya, K.; Tominaga, K. *Chem. Phys. Lett*. **2005**, *411*, 339. (f) Mandal, U.; Adhikari, A.; Dey, S.; Ghosh. S.; Mondal, S. K.; Bhattacharyya, K. *J. Phys. Chem. B* **2007**, *111*, 5896.

(7) (a) Mondal, S. K.; Ghosh, S.; Sahu, K.; Mandal, U.; Bhattacharyya, K. *J. Chem. Phys.* **2006**, *125*, 224710. (b) Ghosh, S.; Dey, S.; Adhikari, A.; Mandal, U.; Bhattacharyya, K. *J. Phys. Chem. B* **2007**, *111*, 7085.

(8) (a) Makarov, V.; Pettitt, B. M.; Feig, M. *Acc. Chem. Res.* **2002**, *35*, 376. (b) Bandyopadhyay, S.; Chakraborty, S.; Bagchi, B. *J. Am. Chem. Soc.* **2005**, *127*, 16660. (c) Bandyopadhyay, S.; Chakraborty, S.; Balasubramanian, S.; Bagchi, B. *J. Am. Chem. Soc.* **2005**, *127*, 4071. (d) Abel, S.; Waks, M.; Urbach, W.; Marchi, M. *J. Am. Chem. Soc.* **2006**, *128*, 382. (e) Heugen, U.; Schwaab, G.; Brundermann, E.; Heyden, M.; Yu, X.; Leitner, D. M.; Havenith, M. *Proc. Natl. Acad. Sci. U.S.A.* **2006**, *103*, 12301.

(9) (a) Pal, S.; Bagchi, B.; Balasubramanian, S. *J. Phys. Chem. B* **2005**, *109*, 12879. (b) Balasubramanian, S.; Pal, S.; Bagchi, B. *Phys. Rev. Lett.* **2002**, *89*, 115505-1-4. (c) Senapati, S.; Berkowitz, M. L. *J. Chem. Phys.* **2003**, *118*, 1937. (d) Faeder, J.; Ladanyi, B. M. *J. Phys. Chem. B*, **2005**, *109*, 6732. (e) Harpham, M. R.; Ladanyi, B. M.; Levinger, N. E. *J. Phys. Chem. B* **2005**, *109*, 16891.

(10) (a) Paul, S.; Chandra, A. *J. Chem. Phys.* **2005**, *123*, 174712. (b) Paul, S.; Chandra, A. *J. Chem. Phys.* **2005**, *123*, 184706. (c) Benjamin, I. *Chem. Rev.* **2006**, *106*, 1212. (d) Michael, D.; Benjamin, I. *J. Chem. Phys.* **2001**, *114*, 2817.

(11) (a) Senapati, S.; Chandra, A. *J. Phys. Chem. B* **2001**, *105*, 5106. (b) Thompson, W. H. *J. Phys. Chem. B* **2005**, *109*, 18201. (c) Li, S. M.; Thompson, W. H. *J. Phys. Chem. B* **2005**, *109*, 4941. (d) W. H. Thompson, *J. Chem. Phys*. **2004**, *120*, 8125. (e) Gomez, J. A.; Thompson, W. H. *J. Phys. Chem. B* **2004**, *108*, 20144. (f) Gulmen, T. S.; Thompson, W. H. *Langmuir* **2006**, *22*, 10919.

(12) (a) Bhargava, B. L.; Devane, R.; Klein, M. L.; Balasubramanian, S. *Soft Matter* **2007**, *3*, 1395. (b) Wang, Y.; Jiang, W.; Yan, T.; Voth, G. A. *Acc. Chem. Res.* **2007**, *40*, 1193. (c) Wang, Y.; Voth, G. A. *J. Am. Chem. Soc.* **2005**, *127*, 12192. (d) Lopes, J. N. A. C.; Padua, A. A. H. *J. Phys. Chem. B* **2006**, *110*, 3330. (e) Triolo, A.; Russina, O.; Bleif, H.-J.; Di Cola, E. *J. Phys. Chem. B* **2007**, *111*, 4641. (f) Hu, Z.; Margulis, C. J. *Proc. Natl. Acad. Sci. U.S.A.* **2006**, *103*, 831. (g) Mandal, P. K.; Sarkar, M.; Samanta, A. *J. Phys. Chem. A* **2004**, *108*, 9048.

(13) (a) Guha, S.; Sahu, K.; Roy, D.; Mondal, S. K.; Roy, S.; Bhattacharyya, K. *Biochemistry* **2005**, *44*, 8940. (b) Cohen, B. C.; McAnaney, T. B.; Park, E. S.; Jan, Y. N.; Boxer, S. G.; Jen, L. Y. *Science* **2002**, *296*, 1700.

(14) (a) Sando, G.; Dahl, K.; Owrutsky, J. C. *J. Phys. Chem. B* **2007**, *111*, 4901. (b) Sando, G. M.; Dahl, K.; Owrutsky, J. C. *Chem. Phys. Lett.* **2006**, *418*, 402. (c) Correa, N. M.; Levinger, N. E. *J. Phys. Chem. B* **2005**, *110*, 13050. (d) Baruah, B.; Roden, J. M.; Sedgwick, M.; Correa, N. M.; Crans, D. C.; Levinger, N. E. *J. Am. Chem. Soc*. **2006**, *128*, 12758.

(15) (a) Grant, C. D.; Steege, K. E.; Bunagan, M. R.; Castner, E. W., Jr. *J. Phys. Chem. B* **2005**, *109*, 22273. (b) Grant, C. D.; DeRitter, M. R.; Steege, K. E.; Fadeeva, T. A.; Castner, E. W., Jr. *Langmuir* **2005**, *21*, 1745.

(c) Humpolickova, J.; Stepanek, M.; Prochazka, K.; Hof, M. *J. Phys. Chem. A* **2005**, *109*, 10803. (d) Frauchiger, L.; Shirota, H.; Uhrich, K. E.; Castner, E. W., Jr. *J. Phys. Chem. B* **2002**, *106*, 7463.

(16) (a) McArthur, E. A.; Eisenthal, K. B. *J. Am. Chem. Soc.* **2006**, *128*, 1068. (b) Nguyen, K. T.; Shang, X. M.; Eisenthal, K. B. *J. Phys. Chem.* **2006**, *110*, 19788.

(17) (a) Maroncelli, M.; Fleming, G. R. *J. Chem. Phys*. **1987**, *86*, 6221. (b) Fee, R. S.; Maroncelli, M. *Chem. Phys*. **1994**, *183*, 235.

(18) Jones, G., II; Jackson, W. R.; Choi, C.-Y.; Bergmark, W. R. *J. Phys. Chem.* **1985**, *89*, 294.

(19) Shirota, H.; Segawa, H. *J. Phys. Chem. A* **2003**, *107*, 3719.

(20) (a) Nandi, N.; Bagchi, B. *J. Phys. Chem. B* **1997**, *101*, 10954. (b) Nandi N.; Bagchi, B. *J. Phys. Chem. A* **1998**, *102*, 8217. (c) Bagchi, B. *Chem. Rev*. **2005**, *105*, 3197. (d) Bhattacharyya, K. *Acc. Chem. Res.* **2003**, *36*, 95.